VOL. 11, NO. 6, MARCH 2016 ISSN 1819-6608
ARPN Journal of Engineering and Applied Sciences

www.arpnjournals.com

SYMMETRICAL SPLIT RING RESONATOR METAMATERIALS FOR MICROWAVE BIOSENSOR

Rammah. A. Alhnomi[1], Z. Zakaria[1], E. Ruslan[2] and A. A. M. Bahar[1]
[1]Centre for Telecommunication Research and Innovation, University Technical Malaysia Melaka, Durian Tunggal, Melaka, Malaysia
[2]Faculty of Technology Engineering, University Technical Malaysia Melaka, Malaysia
E-Mail: alrammah89@gmail.com

ABSTRACT
In this paper, a new type of microwave sensor for determining and detecting the dielectric properties in common solid such as meat is proposed. Various resonators such as coaxial cavity, dielectric, and waveguide resonators have been used for material characterization. However, these resonators are often large in size, expensive, and they have low sensitivity with poor Q-factor. Thus, a new planar resonator technique is presented in order to have higher Q-factor. This type of sensor is based on perturbation theory, in which the dielectric properties of the resonator effect the quality factor and resonance frequency of the microwave resonator. A microstrip of symmetrical split ring resonator (SSRR), which has two gaps, is adopted for the design of the sensor. This resonator is suitable for various industry applications such as food industry, quality control, bio –sensing medicine and pharmacy. A very good agreement is illustrated between the calculated and simulated results at operating frequency of 2.2 GHz. In addition, a high sensitivity is achieved in the same operating resonance frequency by using High Frequency Structure Simulator (HFSS).

Keywords: material characterization, microwave sensors, SSRR.

INTRODUCTION
Microwave sensors are very attractive for a wide range of applications. Recently, microwave technologies play a key role in increasing number of military and industry applications. It is being used in the tunable and switchable filters and oscillators (Gardner *et al.* n.d.; Sun and Zhu 2007; Filters *et al.* 2010), and microwave circuit including antenna and couplers (Chang and Hsieh 2004; Pozar 2012). Chang in (Chang and Hsieh 2004) has developed an equivalent circuit model for the ring resonator when operates near to the lowest resonant frequency by using transmission line theory. The authors in (Alahnomi *et al.* 2015) have studied the microstrip ring resonators based on bio-sensing applications for material characterization and described the performance of different models.

There are various kinds of a biosensor on bio-sensing technologies based on fluorescence (Aoyagi and Kudo 2005), electromechanical transduction (Fritz *et al.* 2000), nano-materials (Guan *et al.* 2005), and surface resonance Plasmon (SPR) (Dostálek *et al.* 2005). Even though these bios-sensors are successful and useful, they often required bulky measurement equipment, complex fabrication steps, time consuming for the processes which make the biological analysis system complex and expensive.

Meat quality evaluation by using dielectric properties has gained more research interest in the past few years. Checking the freshness and quality of the meat has various advantages which are effective, easy, rapid, non-destructive and reliable (Rammah *et al.* 2015). The authors in (Jilani *et al.* 2014) have designed one class of these sensors uses microwave resonant circuits for determining and detecting the dielectric properties of fat contents. In the microwave resonator design, the permittivity of the dielectric substrate has gained an essential role and needs accurate evaluation in different range of frequencies. Various research studies has been focused on meat properties for lower frequencies. Meat quality aspects, quality classes, detection of frozen, chemical contamination and microbial activities has been characterized using the impedance variations of Kilo - Hertz to Mega-Hertz frequency ranges. However, moderately a few literature is found in Giga-Hertz ranges which is mainly focused on the assessment of freshness, salting process, aging state and fat determination (Jilani *et al.* 2014; Jacob *et al.* 2008; Aouabdia *et al.* 2014; Zelenchuk *et al.* 2012; Kılıç *et al.* 2013; Rashidian *et al.* 2012; Zhu *et al.* 2013).

In this paper, symmetrical split ring resonator (SSRR), which is an appropriate component of microwave sensor's performance and enhancement, is presented. This technique has been applied for enhancing the insertion loss and achieving a high Q - factor of the resonator in order to achieve high accuracy, sensitivity and simplicity. This technique is used for the spurious passband at 1st, 2nd, 3rd, and 4th harmonics which is being totally suppressed well above -20 dB of the rejection level and avoiding a visible change in the characteristics of passband filter. Findings and analysis of material measurement technique development are discussed for symmetrical split ring resonators and various factors are considered in order to obtain high accuracy, low cost, easy procedures, and rapid measurement of the desired testing material. The most important of using SSRR is to be used for various industrial applications such as food industry, quality control, bio -sensing medicine and pharmacy.

VOL. 11, NO. 6, MARCH 2016 ISSN 1819-6608
ARPN Journal of Engineering and Applied Sciences

THEORETICAL ANALYSIS OF MICROWAVE BIOSENSOR

Concentric symmetrical split ring resonator was designed on the substrate Roger RT/Duriod 5880 with the thickness of substrate 0.787 mm, and 2.2 of dielectric constant. A total width and length of the substrate are 68 mm and 100 mm, respectively, and fed through with a capacitive microstrip line, satisfying the resonant conditions.

$$2\pi R = n\,\lambda g, \ \text{for } n = 1,2,3 \ldots. \tag{1}$$

Where R is the ring main radius and n is the number of the resonance mode in the harmonic order. The calculated resonance frequency of the harmonic SSRR resonator are 2.2 GHz, 4.4 GHz. 6.6 GHz and 8.8 GHz respectively, with 0.787 mm uniform thickness. These concentric ring resonators were fed through a 0.37 mm capacitive gap between the ring and 34 mm length of the microstrip line. Figure-1 demonstrates the schematic structure of the SSRR with the coupling gap between the ring and feed line, which has to be taken into consideration due to its capacitive effects on changing the resonance significantly. All design parameters of the symmetrical split ring resonator are listed in Table-1.

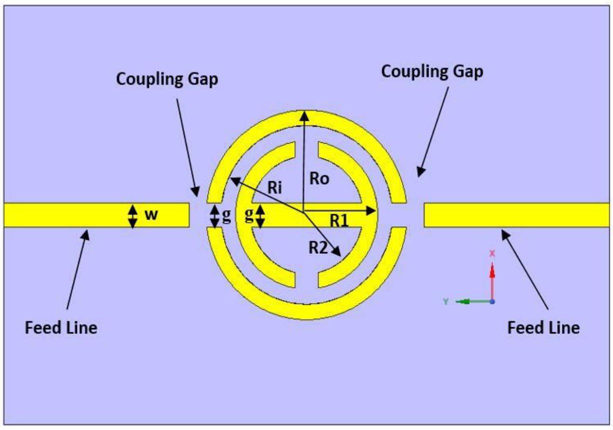

Figure-1. Schematic diagram of the symmetrical split ring design.

The resonant frequencies for the different modes can be calculated in Equation 2.

$$fo = \frac{nc}{2\pi r\sqrt{\varepsilon eff}} \tag{2}$$

c = 3 x 108 m/s.
n = 1, 2, 3,…
r = Radius of the ring.
ε_{eff} = effective permittivity of the substrate.

For the 50 Ω characteristic impedance Zo, the w/d ratio can be found using this formula:

$$\frac{w}{d} = \frac{8e^{A}}{e^{2A}-2} \tag{3}$$

For w/d < 2

$$\varepsilon e = \frac{\varepsilon r-1}{2} + \frac{\varepsilon r-1}{2}\frac{1}{\sqrt{1+\frac{12d}{w}}} \tag{4}$$

Where:

$$A = \frac{Zo}{60}\sqrt{\frac{\varepsilon r+1}{2}} + \frac{\varepsilon r-1}{\varepsilon r+1}\left(0.23 + \frac{0.11}{\varepsilon r}\right) \tag{5}$$

The quality factor (Q-factor) can be determined using this formula:

$$Q = \frac{\omega o}{\Delta\omega} \tag{6}$$

Where ω is the center frequency and Δω is the bandwidth.

Table-1. The parameters design of SSRR.

Parameter	Design value
Substrate: Roger RT/Duriod 5880	**ε= 2.2**
Zo	50 Ω
Lg	100 mm
Wg	68 mm
h	0.787 mm
r	15.85 mm
t	0.0175 mm
w	2.5 mm
l	34 mm
g	0.37 mm

The design structure for the two-port ring resonator with sample; which is illustrated as in Figure-2, has two coupling gaps. This gap is considered as an important part in the ring resonator and it separates the feed lines from the ring which make the structure to support only selective frequencies. The properties of the resonators are often intentionally modified and perturbed by the introduction of small material sample (Pozar 2012). The dielectric sample is placed in a maximum electric field (E-field) region, which produces a reduction in the quality factor (Q-factor) and reduction in the resonant frequency as associated with the loss of the dielectric materials. Together, these can be used for measuring the sample complex relative permittivity.

ARPN Journal of Engineering and Applied Sciences

www.arpnjournals.com

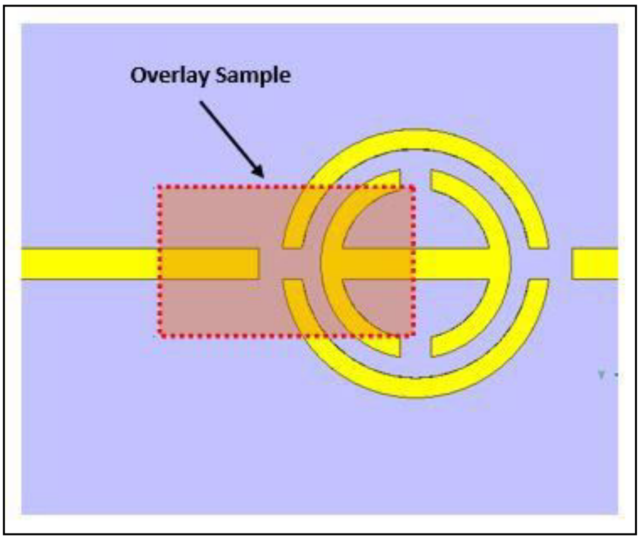

Figure-2. SSRR based on two-ports microstrip resonator with an overlay sample.

RESULT AND DISCUSSIONS

From the simulation result, the effect of the coupling-gaps in resonant frequency is demonstrated in Figure-3. The coupling gap is varied between the ranges of 150 µm to 650 µm. It can be observed that the performance of the resonator is dependent on the size of the coupling gap. When the used size is very small, a lower loss will occur, but it affects the fields in the resonant structure. Besides, a larger gap size will result more losses but less field perturbation.

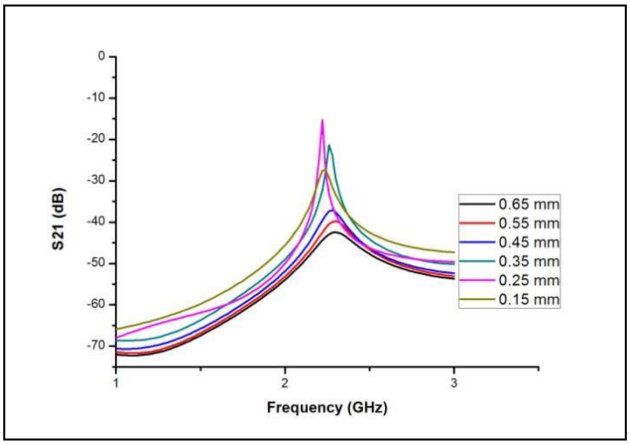

Figure-3. The effect of the coupling-gaps on resonant frequency.

For the simulated result, Figure-4 and 5 illustrate the simulated transmission (S21) and reflected (S11) parameters of the symmetrical split ring resonator before and after optimization. It demonstrates that the fundamental frequency is at 2.2 GHz and the second harmonic frequency is at 4.62 GHz and then third is at 6.6 GHz and the last resonance is occurred at 8.76 GHz for unloaded condition resonator. The fundamental frequency obtained from the simulated result is found in good agreement with the calculation in Equation 2.

The Q-factor in the loose coupling has a lower value at the first mode comparatively with other modes before the optimization was made. Table-2 indicates the comparison before and after optimization of the designed resonator in terms of Q-factor, transmission S21 (dB), and reflection S11 (dB). It can be observed that the Q-factor has been increased to 407.34 at 2.22 GHz compared to 33.89 at 2.26 GHz before optimization. This demonstrates that, a small gap produces high Q-factor of the SSRR. This could be due to the coupling loss of the gaps between the feed lines and ring resonator and a small coupling gap also produces a maximum field.

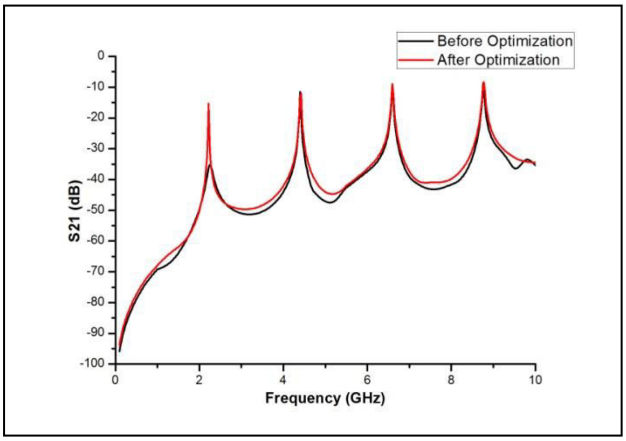

Figure-4. The simulated transmission (S21) of SSRR.

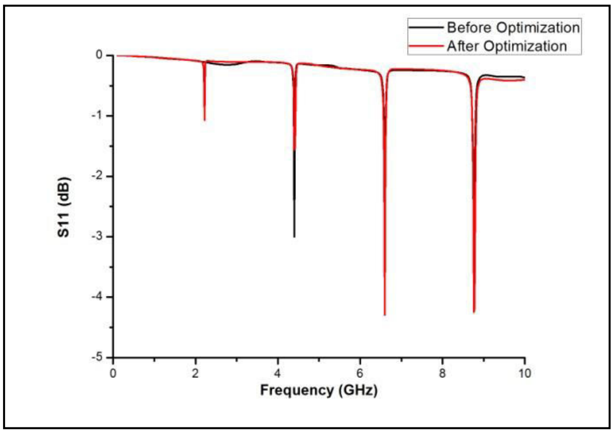

Figure-5. The simulated reflected (S11) of SSRR.

ISSN 1819-6608
ARPN Journal of Engineering and Applied Sciences

www.arpnjournals.com

Table-2. The values of the Q-factor, S21, S11 of the SSRR.

Mode (n)	Before optimization				After optimization			
	Frequency (GHz)	Q-Factor	S11 (dB)	S21 (dB)	Frequency (GHz)	Q-Factor	S11 (dB)	S21 (dB)
1	2.26	33.98	-0.12	-35.19	2.22	407.34	-1.07	-15.32
2	4.40	517.65	-2.99	-11.61	4.42	243.53	-1.56	-12.03
3	6.60	379.31	-3.78	-10.09	6.60	368.72	-4.29	-8.99
4	8.76	369.62	-3.74	-9.66	8.76	302.07	-4.25	8.64

The coupling efficiency between the feed lines and ring resonator is determined by their cross section and separation (Gap Size). Figure-6 illustrates the effects of the coupling gap in the Q-factor of the resonator. A low coupling loss is having a high quality (Q) factor and less insertion loss for high performance. As the gap increases, the Q-factor decreases which affects the performance of the ring. The coupling Q-factor between the feed line and resonator is larger than 400 for a gap size of 0.25 mm.

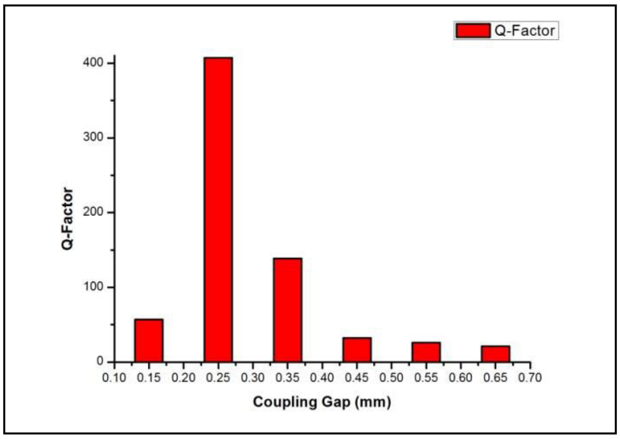

Figure-6. The effect of coupling gap in Q-factor.

For loaded condition, an overlay meat sample with 0.787 mm thickness is used in order to determine the behavior of the resonant frequency. From the simulation, a frequency shift of a 2.2 GHz resonance in the presence of the overlay sample is observed at 18 %. Comparison between the simulation result of unloaded and loaded with an overlay sample for the resonant frequency is illustrated in Figure-7. It indicates the frequency shift to lower frequency when the overlay sample is used. This is due to the maximum electric field of the resonator when it is perturbed to the sample and more fringing fields is focused into the overlay sample. Not only the shifting of frequency can be seen, but also there is a variation in dB level when the overlay sample is applied and this is because of the effective dielectric constant. As a result, the effective permittivity has a direct proportional to the thickness of the overlay sample.

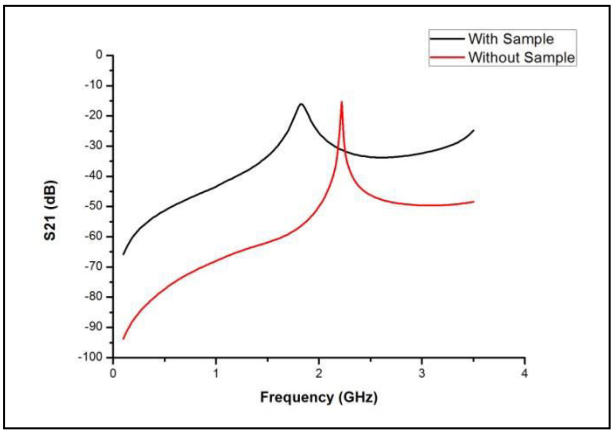

Figure-7. Comparison between the simulation result of unloaded and loaded with an overlay sample.

CONCLUSIONS

In this paper, a microwave bio-sensor investigation based on a dielectric loaded microstrip symmetrical split ring resonator is performed and proposed as a viable candidate for microwave sensor's performance and enhancement. The design is simulated and tested an overlay sample by using HFSS simulator. The coupling gap between the ring and feed lines was varied and the result was obtained and recorded. This design exhibits the lowest insertion loss with a high Q - factor of the ring resonator. For further improvements, the possibility of decreasing the size of the coupling gap is recommended or using an enhancement method in order to improve the performance of the Symmetrical split ring resonator. The proposed ring resonator has a sample structure, easy fabrication, cost effective and easy to enhance the sensor's performance with respect to the material characterization. This resonator is suitable for various industry applications such as food industry, quality control, bio -sensing medicine and pharmacy. Future work can be done by verifying and validating the simulated results through experimental works.

REFERENCES

A.A. Rammah, Z. Zakaria, E. Ruslan, A.A.M., I., 2015. Comparative Study of Materials Characterization using

Microwave Resonators. Aust. J. Basic and Appl. Sci., 9(January), pp. 76-85.

Alahnomi, R.A. Zakaria, Z., Ruslan, E., and Esa, A. A. M., 2015. Optimization Analysis of Microwave Ring Resonator for Bio-sensing Application, International Journal of Applied Engineering Research.

Aouabdia, N., Belhadj-Tahar, N.E. and Alquie, G. 2014. Rectangular patch resonator sensors for characterization of biological materials. 2014 IEEE 11th International Multi-Conference on Systems, Signals and Devices (SSD14), pp. 1-4. Available at: http://ieeexplore.ieee.org/lpdocs/epic03/wrapper.htm?arnumber=6808748.

Aoyagi, S. and Kudo, M. 2005. Observation of fluorescence-labeled protein A on a biosensor surface by means of TOF-SIMS. Sensors and Actuators B: Chemical, 108(1-2), pp. 708-712. Available at: http://linkinghub.elsevier.com/retrieve/pii/S0925400504008731.

Chang, K. and Hsieh, L.H. 2004. Microwave Ring Circuits and Related. John Wiley and Sons.

Dostálek, J., Vaisocherová, H. and Homola, J. 2005. Multichannel surface plasmon resonance biosensor with wavelength division multiplexing. Sensors and Actuators B: Chemical, 108(1-2), pp. 758-764. Available at: http://linkinghub.elsevier.com/retrieve/pii/S0925400505000493.

Srisathit, K., Worapishet, A., and Surakampontorn, W. 2010. Design of Triple-Mode Ring Resonator for Wideband Microstrip Bandpass Filters. 58(11), pp. 2867-2877.

Fritz, J., Baller, M. K., Lang, H. P., Rothuizen, H., Vettiger, P., Meyer, E., Guntherodt, H.-J., Gerber, CH. and Gimzewski, J.K. 2000. Translating Biomolecular Recognition into Nanomechanics. 288(April), pp. 316-318.

Gardner, P., Paul, D.K. and Tan, K.P., Planar microstrip Ring Resonator Filters. pp. 1-6.

Guan, W.-J. Li, Y., Chen, Y-Q., Zhang, X-B., and Hu, G-Q., 2005. Glucose biosensor based on multi-wall carbon nanotubes and screen printed carbon electrodes. Biosensors and bioelectronics, 21(3), pp. 508-12. Available at: http://www.ncbi.nlm.nih.gov/pubmed/16076441.

Jacob, M.V., Thomas, S., Sebastian, and M., Mazierska, J., 2008. Low temperature microwave characterisation of greentapes using Split Post Dielectric Resonator. 2008 Asia-Pacific Microwave Conference, 2, pp. 1-4. Available at: http://ieeexplore.ieee.org/lpdocs/epic03/wrapper.htm?arnumber=4958678.

Jilani, M.T., Zakariya, M.A. and Cheong, L.Y., 2014. Dielectric method for determination of fat content at 1 GHz frequency. 2014 5th International Conference on Intelligent and Advanced Systems (ICIAS), pp. 1-4. Available at: http://ieeexplore.ieee.org/lpdocs/epic03/wrapper.htm?arnumber=6869463.

Kılıç, E., Siart, U., Wiedenmann, O., Faz, U., Ramakrishnan, R., Saal, P., and Eibert, T. F., 2013. Cavity Resonator Measurement of Dielectric Materials Accounting for Wall Losses and a Filling Hole. 62(2), pp. 401-407.

Pozar, D.M., 2012. Microwave Engineering Fourth Edi., Rashidian, A., Aligodarz, M. and Klymyshyn, D., 2012. Dielectric characterization of materials using a modified microstrip ring resonator technique. IEEE Transactions on Dielectrics and Electrical Insulation, 19(4), pp. 1392-1399. Available at: http://ieeexplore.ieee.org/lpdocs/epic03/wrapper.htm?arnumber=6260016.

Sun, S. and Zhu, L., 2007. Wideband Microstrip Ring Resonator Bandpass Filters under Multiple Resonances. 55(10), pp. 2176-2182.

Zelenchuk, D.E., Fusco, V., Mendez, A., and Linton, D., 2012. Millimeter-Wave Printed Circuit Board Characterization Using Substrate Integrated Waveguide Resonators. 60(10), pp. 3300-3308.

Zhu, X.-C., Hong, W., Wu, K., Tang, H-J., Hao, Z-C., and Zhou, H-X., 2013. Characterization of substrate material using complementary split ring resonators at terahertz frequencies. 2013 IEEE International Wireless Symposium (IWS), pp. 1-4. Available at: http://ieeexplore.ieee.org/lpdocs/epic03/wrapper.htm?arnumber=6616829.